

## Digital Hadron Calorimetry

To cite this article: Burak Bilki 2018 *JINST* **13** C03012

View the [article online](#) for updates and enhancements.

### Related content

- [Resistive Plate Chambers for imaging calorimetry — The DHCAL](#)  
J Repond
- [Tests of a Digital Hadron Calorimeter](#)  
Burak Bilki, John Butler, Ed May et al.
- [Construction and performance of a silicon photomultiplier/extruded scintillator tail-catcher and muon-tracker](#)  
C Adloff, J Blaha, J -J Blaising et al.



**IOP | ebooks™**

Bringing you innovative digital publishing with leading voices to create your essential collection of books in STEM research.

Start exploring the collection - download the first chapter of every title for free.

CHEF2017 — CALORIMETRY FOR THE HIGH ENERGY FRONTIER  
2–6 OCTOBER 2017  
LYON, FRANCE

## Digital Hadron Calorimetry

---

**Burak Bilki,<sup>a,b</sup> on behalf of the CALICE Collaboration**

<sup>a</sup>University of Iowa, Iowa City, IA, U.S.A.

<sup>b</sup>Beykent University, Istanbul, Turkey

E-mail: [Burak.Bilki@cern.ch](mailto:Burak.Bilki@cern.ch)

**ABSTRACT:** The Particle Flow Algorithms attempt to measure each particle in a hadronic jet individually, using the detector providing the best energy/momentum resolution. Therefore, the spatial segmentation of the calorimeter plays a crucial role. In this context, the CALICE Collaboration developed the Digital Hadron Calorimeter.

The Digital Hadron Calorimeter uses Resistive Plate Chambers as active media and has a 1-bit resolution (digital) readout of  $1 \times 1 \text{ cm}^2$  pads. The calorimeter was tested with steel and tungsten absorber structures, as well as with no absorber structure, at the Fermilab and CERN test beam facilities over several years. In addition to conventional calorimetric measurements, the Digital Hadron Calorimeter offers detailed measurements of event shapes, rigorous tests of simulation models and various tools for improved performance due to its very high spatial granularity.

Here we report on the results from the analysis of pion and positron events. Results of comparisons with the Monte Carlo simulations are also discussed. The analysis demonstrates the unique utilization of detailed event topologies.

**KEYWORDS:** Calorimeter methods; Detector modelling and simulations I (interaction of radiation with matter, interaction of photons with matter, interaction of hadrons with matter, etc); Resistive-plate chambers

---

## Contents

<b>1</b>	<b>Introduction</b>	<b>1</b>
<b>2</b>	<b>Fe-DHCAL measurements at Fermilab Test Beam Facility</b>	<b>2</b>
<b>3</b>	<b>W-DHCAL measurements at CERN</b>	<b>3</b>
<b>4</b>	<b>Min-DHCAL measurements at Fermilab Test Beam Facility</b>	<b>4</b>
<b>5</b>	<b>Conclusions</b>	<b>6</b>

---

## 1 Introduction

The High Energy Physics community has come to a consensus that the achievement of the high precision measurements aimed in future experiments, such as the ones envisaged at the International Linear Collider (ILC) [1], Compact Linear Collider (CLIC) [2] and Future Circular Collider (FCC) [3], can be made possible with the utilization of the Particle Flow Algorithms (PFAs) [4]. A detector optimized for the implementation of PFAs requires calorimeters with extremely fine segmentation of the readout to separate showers from charged and neutral particles. In this context, the CALICE collaboration [5] developed several high segmentation calorimeters.

The large Digital Hadron Calorimeter (DHCAL) prototype was built in 2008–2010, following the successful completion of the test beam program of a small size prototype. The latter produced a number of interesting results [6] and served as basis for the design of the DHCAL.

The DHCAL uses Resistive Plate Chambers (RPCs) as active media and is read out with  $1 \times 1 \text{ cm}^2$  pads and 1-bit resolution (digital). A single layer of the DHCAL measures roughly  $1 \times 1 \text{ m}^2$  and consists of  $96 \times 96$  pads. The active layers were placed between different absorber structures, to be described in detail below. In addition to the absorber plates, each layer of RPCs was contained in a cassette with a 2 mm thick Copper front plate and a 2 mm thick Steel back plate. The details of the DHCAL are given in [7].

In order to obtain a unique dataset of electromagnetic and hadronic interactions with unprecedented spatial resolution, the DHCAL went through a broad test beam program. The DHCAL was tested with steel and tungsten absorber structures, as well as with no absorber structure, at Fermilab and CERN test beam facilities over several years. In addition to conventional calorimetric measurements, the DHCAL offers detailed measurements of event shapes, rigorous tests of simulation models and various tools for improved performance due to its very high spatial granularity.

Here, we report on basic calorimetric measurements, such as response linearity and energy resolution under various test conditions and also present detailed measurements of the electromagnetic and hadronic shower shapes. Results of comparisons with the Monte Carlo simulations are also reported.

## 2 Fe-DHCAL measurements at Fermilab Test Beam Facility

Fermilab Test Beam Facility (FTBF) [8] delivers 120 GeV primary protons and 1–60 GeV secondary beams that are composed of muons, pions and positrons (electrons). The beam is delivered once every minute in spills lasting 3.5 seconds. The intensity of the beam can be adjusted to accommodate the needs of different detectors. Due to the limited rate capability of (glass) RPCs [6, 9], the DHCAL requested rates between 50 to 200 Hz/cm<sup>2</sup>, depending on the momentum selection.

During these tests at FTBF, up to 52 layers were installed. The calorimeter consisted of a 38-layer main stack with 1.75 cm thick steel absorber plates and a 14-layer tail catcher with eight 2 cm thick steel plates followed by six 10 cm thick steel plates. This test setup is called the “Fe-DHCAL”.

The data acquisition for the broadband muon beam, which was used to measure the performance parameters of the RPCs, i.e. the efficiency and average pad multiplicity, was triggered by the coincidence of two large 1 × 1 m<sup>2</sup> scintillator paddles located one in front of the DHCAL and one in the back of the tail catcher. The mixed secondary beam and primary proton events were triggered by the coincidence of two 20 cm × 20 cm scintillator paddles located upstream of the DHCAL stack. The beam line houses Čerenkov detectors for particle identification for the mixed secondary beam.

The DHCAL data contain the hit position information, the time stamp of the individual hits and the time stamp from the trigger and timing unit. Additionally, discriminated signals from a beam Čerenkov counter and a muon tagger (the downstream scintillator 1 × 1 m<sup>2</sup> paddle) are integrated into the data stream by the data acquisition system. The event selection requires at least five active layers (layers with at least one hit) in order to eliminate events with spurious triggers e.g. by cosmic rays.

The calibration of the DHCAL involves several steps. To begin, the performance parameters of the individual RPCs, i.e. the efficiency and the average pad multiplicity, are measured. Muon events or track segments in hadronic interactions are used to obtain these parameters. In a second step, the number of hits measured in a given RPC is corrected for differences in its performance parameters. Three different approaches have been explored: full calibration, density-weighted calibration, and hybrid calibration. Implementation details of the calibration procedures can be found in [10].

Figure 1 (left) shows the response of the Fe-DHCAL to pions of energies from 2 to 60 GeV. The uncalibrated data is shown as black circles and the results of density-weighted calibration are shown in green squares. The points are fit empirically to  $N = aE^m$  where  $N$  is the average number of hits,  $E$  is the beam energy,  $a$  is the slope and  $m$  is the power term that denotes the extent of linearity of the response. The uncalibrated response shows 4% non-linearity and the density-weighted calibration improves the non-linearity to 2%. Fe-DHCAL is compensating at around 8 GeV. At lower energies, Fe-DHCAL is under-compensating with larger response to electromagnetically interacting particles than hadrons, whereas for higher energies it is over-compensating (please see the conference talk for the visual description). Figure 1 (right) shows the hadronic energy resolution of the Fe-DHCAL. It should be noted here that no containment cuts or correction for response non-linearity were applied to the data at that stage. The points are fit to  $\sigma(N)/N = \alpha/\sqrt{E} \oplus C$  where  $\alpha$  is the stochastic term and  $C$  is the constant term. Both the fit to the uncalibrated data (black) and to the density-weighted calibration data (green) are up to and including 25 GeV point. The fits are then extrapolated to 60 GeV. The stochastic term is 66% (64%) and the constant term is 4% (3%) for the uncalibrated (density-weighted calibration) data.

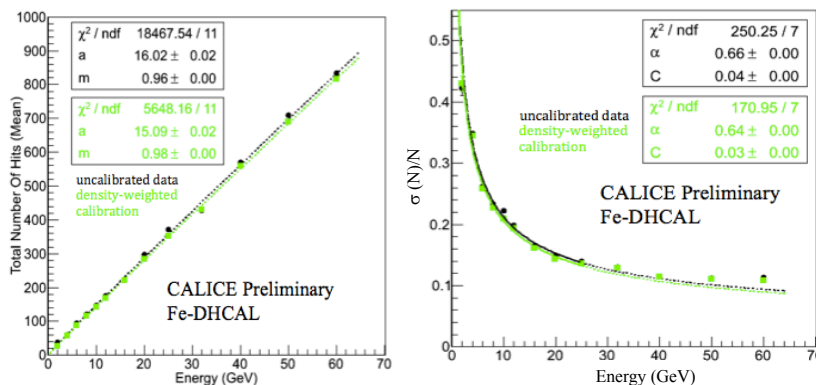


**Figure 1.** The response of the Fe-DHCAL to pions (left) and the hadronic energy resolution (right).

### 3 W-DHCAL measurements at CERN

The “W-DHCAL” consisted of 54 active layers interleaved with Tungsten absorber plates [11]. The first 39 of these layers were inserted into the CERN tungsten absorber structure [12], featuring 1 cm thick tungsten plates and in the following named the main stack. The distance between the plates was 15 mm, of which 12.85 mm were occupied by the cassette structure of the active layers. The remaining 15 layers were inserted into a steel structure, the tail catcher, which was located 23.5 cm behind the main stack. The total thickness of the 54-layer W-DHCAL (main stack and tail catcher) corresponded to approximately 183 radiation lengths or 11.1 nuclear interaction lengths.

The PS beam line offers beam in the momentum range of 1–10 GeV/c [13]. The particles arrived in 400 millisecond spills. During the two week run period, the number of spills per 45 second intervals varied from one to three. The SPS beam line offers beam in the momentum range of 10–300 GeV/c [13]. The particles arrive in 9.7 second spills every 45–60 seconds.

Figure 2 (left) shows the mean response as function of beam energy for the various particles in the beam. As the response of individual RPCs as function of time has not yet been calibrated, the response of through-going muons shows some fluctuations. The responses to positive pions, negative pions and protons (after correction for the rest mass) show reasonable agreement. The response to electrons and positrons is significantly smaller than the response to hadrons. In other words, the W-DHCAL with  $1 \times 1 \text{ cm}^2$  readout pads is strongly overcompensating, even at these low energies which is in contrast to what was observed with Fe-DHCAL, where the response is compensating in the range of 8–10 GeV/c and under- (over-) compensating below (above). The response to electrons, pions and protons was fit empirically with a power law,  $N = aE^m$ . The value of  $m$  for hadrons is 0.90 and for electrons 0.78 which indicate a non-linearity of 10% for hadrons and 22% for electrons.

Figure 2 (middle) shows the resolution defined as relative width of the Gaussians versus beam energy. The widths for both electrons and pions have been corrected for the observed non-linearity of the response. As expected, the through-going muon response shows a constant width, independent of the momentum selection. At momenta below 6 GeV/c the pion distributions showed small, asymmetric tails (decreasing with higher momenta), which were excluded from the fit ranges. The hadron (electron) response shows the characteristic behavior of calorimeters with 68.0% (29.4%) stochastic term and 5.4% (16.6%) constant term.

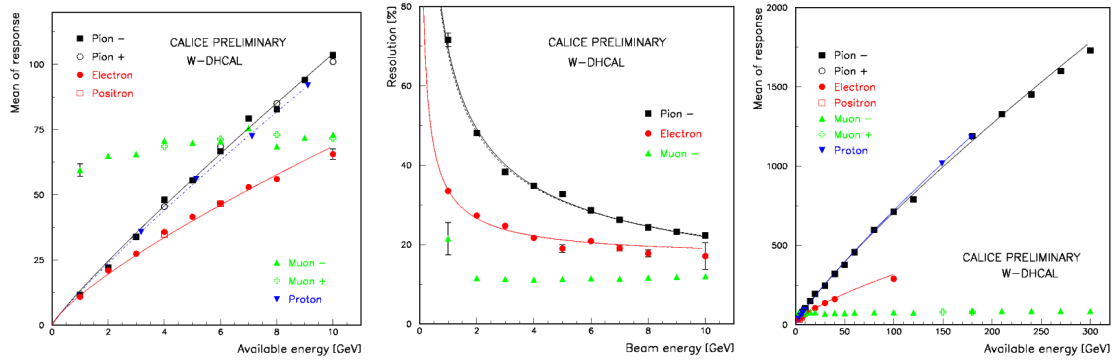


**Figure 2.** Mean response as function of beam energy (left); hadronic and electromagnetic energy resolution of W-DHCAL in the energy range of 1–10 GeV (middle); the mean response as function of beam energy over the entire momentum/energy range of the PS and SPS beam lines (right).

The mean response as function of beam energy over the entire momentum/energy range of the PS and SPS is shown in figure 2 (right). The effects of saturation noted with the PS data are also visible at higher energies. Empirical fits to a power law seem to describe the data adequately with  $(a, m) = (14.7, 0.84)$  for pions and  $(12.7, 0.70)$  for electrons.

At a given momentum, the average number of hits is significantly smaller with tungsten than with steel absorber plates, of the order of 30% less. The response to pions (and electrons) deviates from a straight line already at low momenta (i.e. below 10 GeV/c). This is due to the higher density of showers in tungsten absorbers. These effects can be mitigated with smaller readout pad sizes. The resolutions are also somewhat inferior to what was obtained with steel plates. Software compensation techniques, successfully applied to the CALICE AHCAL data [14], are expected to improve both the linearity and the resolutions.

#### 4 Min-DHCAL measurements at Fermilab Test Beam Facility

In special tests, 50 active layers of the DHCAL were exposed to low energy particle beams, without being interleaved by absorber plates. The thickness of each layer corresponded approximately to 0.29 radiation lengths or 0.034 nuclear interaction lengths. This minimal absorber material configuration is called the “Min-DHCAL” [15].

The Min-DHCAL was exposed to the test beam at FTBF. Runs were taken with a selected momentum in the range of 1–10 GeV/c. The simulation of the test beam set-up is based on the GEANT4 version 10.02 with default parameters and FTFP\_BERT\_EMY physics list [16]. Any energy deposition generated by the simulation in the gas gap of the RPCs is used as a seed for creating an avalanche. The response of the RPCs is simulated using a standalone program, called RPC\_sim [6].

Figure 3 shows the average longitudinal shower shape (left); the radial distance of each hit to the fitted straight line intersecting the corresponding detector plane (middle); and the distribution of the density of hits, defined as the number of hits in a volume of  $3 \times 3 \times 3$  pads surrounding the hit, (right) for 6 GeV positrons. The longitudinal shower shape obtained with the simulation shows reasonable agreement. Apart from a small depletion at small radii in the data, satisfactory

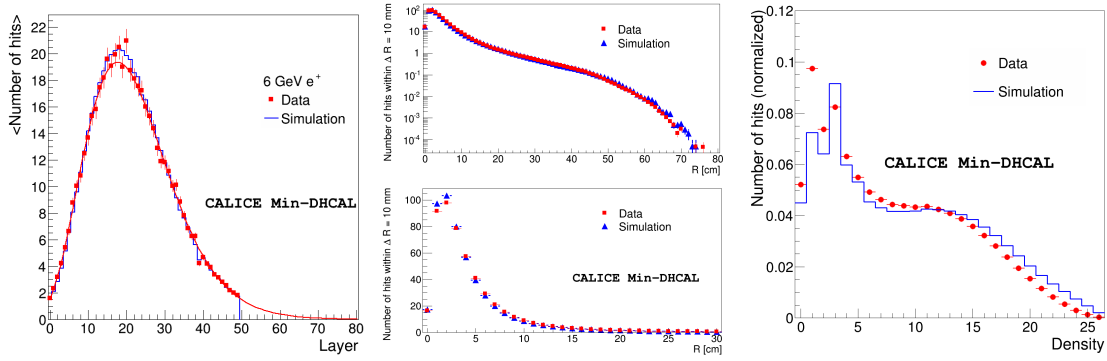


**Figure 3.** For 6 GeV positrons: longitudinal shower shape (left); the distribution of the radial distance of hits from shower axis in logarithmic/linear y-scale in upper/lower panels (middle); distribution of the density of hits (right), data (red) and simulation (blue).

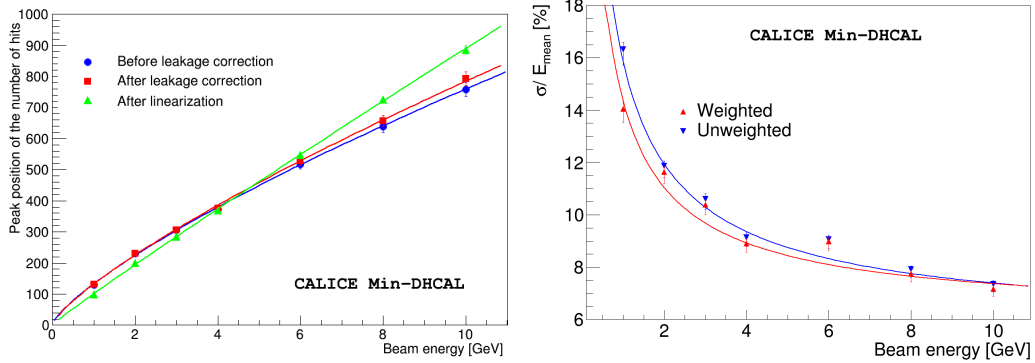


**Figure 4.** Measured peak position of the number of hits for positrons as a function of beam energy: before any correction (blue), after leakage corrections (red) and after linearization of the response based on the hit densities (green) (left); energy resolution versus beam energy for positrons: before (blue) and after (red) the linearization procedure (right).

agreement is observed over the entire range of the radial shower shape. The simulation shows a higher probability for higher hit densities than the data, possibly indicating a still persistent lack of multiple scattering modelling in the simulation.

The high spatial segmentation of the imaging calorimeters allow the application of corrections to the measured number of hits which might result in an improved linearity of the response and energy resolution [14]. The DHCAL data can be corrected for leakage using the detailed shower profiles, and the response can be linearized by assigning different weights to hits based on their densities. Figure 4 (left) shows the response as a function of beam energy before any corrections (blue), after leakage correction (red) and after linearization (green). The effects of the procedures are clearly visible. The  $m$  values from the fits to the power law are  $0.76 \pm 0.02$  before corrections and  $0.94 \pm 0.01$  after linearization. Figure 4 (right) shows the energy resolution as a function of beam energy obtained both before (blue) and after (red) the linearization procedure. The density-weighted linearization procedure results in a modest improvement of about 10%. The stochastic terms obtained before and after the linearization procedure are  $14.8 \pm 0.4$  and  $13.0 \pm 0.4$  respectively.

## 5 Conclusions

The first Digital Hadron Calorimeter was built and tested successfully. By construction, the DHCAL was the first large-scale calorimeter prototype with embedded front-end electronics, digital readout, pad readout of Resistive Plate Chambers and extremely fine segmentation.

Fine segmentation allows the study of electromagnetic and hadronic interactions with unprecedented level of spatial detail, and the utilization of various techniques not implemented in the community so far e.g. software compensation and leakage correction.

Standard Geant4 simulation package fails to reproduce data well. Some optional packages allow big improvement in the agreement. The disagreements are at the very fine level of detail which is not available in conventional calorimeters.

The concept of Digital Hadron Calorimetry is validated.

## References

- [1] <https://www.linearcollider.org/ILC>.
- [2] <http://clic-study.web.cern.ch/>.
- [3] <https://fcc.web.cern.ch/Pages/default.aspx>.
- [4] CALICE collaboration, C. Adloff et al., *Tests of a particle flow algorithm with CALICE test beam data*, 2011 *JINST* **6** P07005 [[arXiv:1105.3417](https://arxiv.org/abs/1105.3417)].
- [5] <https://twiki.cern.ch/twiki/bin/view/CALICE/WebHome>.
- [6] G. Drake, J. Repond, D.G. Underwood and L. Xia, *Resistive Plate Chambers for hadron calorimetry: Tests with analog readout*, *Nucl. Instrum. Meth. A* **578** (2007) 88;  
B. Bilki et al., *Calibration of a digital hadron calorimeter with muons*, 2008 *JINST* **3** P05001 [[arXiv:0802.3398](https://arxiv.org/abs/0802.3398)];  
B. Bilki, J. Butler, G. Mavromanolakis, E. May, E. Norbeck, J. Repond et al., *Hadron Showers in a Digital Hadron Calorimeter*, 2009 *JINST* **4** P10008 [[arXiv:0908.4236](https://arxiv.org/abs/0908.4236)];  
B. Bilki, J. Butler, E. May, G. Mavromanolakis, E. Norbeck, J. Repond et al., *Measurement of the Rate Capability of Resistive Plate Chambers*, 2009 *JINST* **4** P06003 [[arXiv:0901.4371](https://arxiv.org/abs/0901.4371)];  
B. Bilki, J. Butler, E. May, G. Mavromanolakis, E. Norbeck, J. Repond et al., *Measurement of Positron Showers with a Digital Hadron Calorimeter*, 2009 *JINST* **4** P04006 [[arXiv:0902.1699](https://arxiv.org/abs/0902.1699)];  
B. Bilki, J. Butler, E. May, G. Mavromanolakis, E. Norbeck, J. Repond et al., *Environmental Dependence of the Performance of Resistive Plate Chambers*, 2010 *JINST* **5** P02007 [[arXiv:0911.1351](https://arxiv.org/abs/0911.1351)].
- [7] C. Adams et al., *Design, construction and commissioning of the Digital Hadron Calorimeter — DHCAL*, 2016 *JINST* **11** P07007 [[arXiv:1603.01653](https://arxiv.org/abs/1603.01653)].
- [8] <http://ftbf.fnal.gov/>.
- [9] M. Affatigato et al., *Measurements of the rate capability of various Resistive Plate Chambers*, 2015 *JINST* **10** P10037.
- [10] CALICE Analysis Note, CAN-042, 2013.
- [11] CALICE Analysis Note, CAN-039, 2012.
- [12] CALICE Analysis Note, CAN-036, 2012.

- [13] <http://sba.web.cern.ch/sba/>.
- [14] C. Adloff et al., *Hadronic energy resolution of a highly granular scintillator-steel hadron calorimeter using software compensation techniques*, *2012 JINST* **7** P09017 [[arXiv:1207.4210](#)].
- [15] B. Freund et al., *DHCAL with Minimal Absorber: Measurements with Positrons*, *2016 JINST* **11** P05008 [[arXiv:1603.01652](#)].
- [16] GEANT4 collaboration, S. Agostinelli et al., *GEANT4: A Simulation toolkit*, *Nucl. Instrum. Meth. A* **506** (2003) 250.